JOURNAL OF PROPULSION AND POWER
Vol. 15, No. 2, March–April 1999

Disk Temperature Details of Rim Seal Turbulent Heat Diffusion and Disk Frictional Heating

S. H. Ko*
Chungnam National University, Taejon 305-764, Republic of Korea
and
D. L. Rhode†
Texas A&M University, College Station, Texas 77843

Heating from rim seal ingress and disk friction were numerically investigated using the simplified subproblem approach that excludes the mainstream complexities caused by the presence of vanes and blades, as well as other asymmetries. The combined effects of Re_θ and C_w on the blade-root/disk temperatures were analyzed. The elliptic, two-dimensional axisymmetric Navier–Stokes equations were solved at typical engine temperatures, pressures, and flow rates using adiabatic surfaces. For an axisymmetric, axial clearance rim seal without mass ingress, it was found that the intense τ_{rx} from the mainstream produces extremely high-turbulence kinetic energy. This extremely high-turbulence energy at the mainstream-rim seal interface gives high-turbulence heat diffusion ingress without mass ingress. It was also found that turbulent heat diffusion ingress is dominant over disk frictional heating for Re_θ values near half of the engine nominal value. Further, it was found that it is the high values of Re_θ that gives high gap recirculation zone temperatures, but sufficient disk centrifugal pumping to reduce the area for heat convection between the gap recirculation zone and the blade-root surface.

Nomenclature

C_w = volumetric flow rate parameter, $Q/(\nu R)$
c = stator shroud gap axial width
H = stagnation enthalpy
k = total turbulent kinetic energy, $k^{(1)} + k^{(2)}$
$k^{(1)}$, $k^{(2)}$ = partial turbulence kinetic energies
L_e = characteristic length scale
P = turbulence energy production
Q = volumetric purge flow rate
R = radius of disk
$Re_{x,m}$ = axial Reynolds number of mainstream, $(2UH)/\nu$
Re_θ = rotational Reynolds number of disk, $(\Omega R^2)/\nu$
$Re_{\theta,m}$ = rotational Reynolds number of mainstream, $(2WH)/\nu$
R_i = radius of cooling air inlet slit into cavity
s = axial width of cavity
T = temperature
T^* = normalized temperature, $(T - T_2)/(T_1 - T_2)$
U, V, W = mean velocities in x, r, and θ directions
x_i = spatial coordinate in tensor notation
x, r, θ = axial, radial, and tangential coordinates
$\varepsilon^{(1)}$, $\varepsilon^{(2)}$ = turbulence energy transfer rates
μ = absolute viscosity
ν = kinematic viscosity
ρ = fluid density
Ω = rotational speed

Subscripts
1 = mainstream
2 = cooling purge flow

Superscripts
(1) = production zone of turbulent kinetic energy spectrum
(2) = transfer zone of turbulent kinetic energy spectrum
* = nondimensionalized

Introduction

IT is well known that the ingress of hot mainstream gas into a turbine wheelspace cavity can seriously raise, e.g., the blade-root and disk temperatures. This is an important reliability concern. Because of a lack of detailed understanding of several very complex ingress/egress phenomena, progress toward improved seal configurations has been hindered. Also, an unnecessarily high sacrificial purge flow has been typically tolerated. The rotor–stator cavity purge throughflow proceeds radially outward, being centrifugally pumped by the disk. Figure 1 shows the generalized wheelspace cavity and rim seal along with the computational domain. The stationary shroud, in close proximity to the rotor, forms the axial-clearance rim seal through which the purge throughflow discharges into the mainstream.

Phadke and Owen[1–3] conducted comprehensive testing of models that include a mainstream, whereas many investigations focused on a simplified subproblem that excludes the presence of the mainstream. They explained a contradiction of Re dependence that stems from the existence of both a rotation-dominated (high Re_θ) ingress flow regime and an external-flow-dominated (high $Re_{x,m}$) ingress regime. For the latter case, pressure asymmetries in the mainstream caused significant circumferential variation of pressure drop across the seal, and hence, local mass ingress. For the external-flow-dominated regime, mainstream pressure asymmetry effects from various sources were observed by Campbell,[4] and their significance was confirmed by Abe et al.,[5] Kobayashi et al.,[6] Phadke and Owen,[3] Dadkhah et al.,[7] and Hamabe and Ishida.[8] These mainstream asymmetries were caused by guide vanes or other flow disturbances. Additional information is provided by Owen and Rogers.[9]

Received May 5, 1997; revision received Sept. 24, 1998; accepted for publication Oct. 16, 1998.

*Assistant Professor, Department of Mechanical Design Engineering, 220, Kung-dong, Yusong gu.
†Professor, Mechanical Engineering Department. E-mail: drhode@mengr.tamu.ed. Member AIAA.

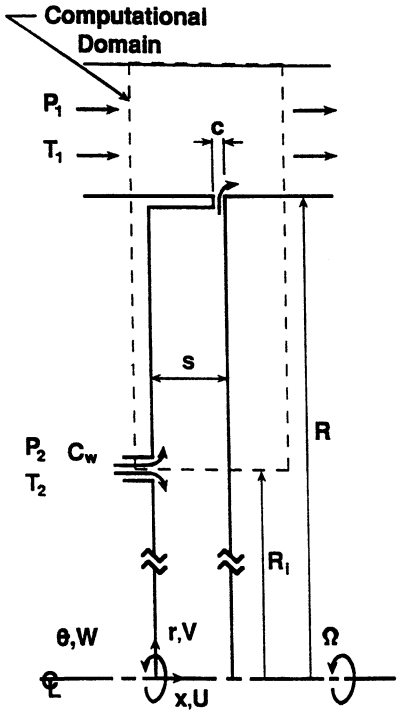

Fig. 1 Idealized computational domain of turbine rim cavity.

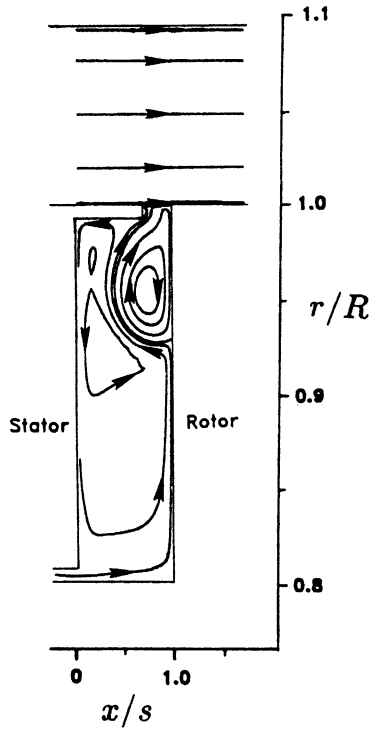

Fig. 2 Streamlines showing the GRZ near the rim seal gap region for C_w = 7200 and $Re_\theta = 7.62 \times 10^6$.

Regarding computational work, the only solutions of rim seal–mainstream interaction, with vanes included in the mainstream, are by Chew et al.,[10] using the mixing-length turbulence model. They considered incompressible flow in which the effect of vanes was approximately simulated by using mainstream inlet values taken from a previous vane trailing-edge potential flow solution. The solution showed local ingress in the vane wake (where high mainstream pressure occurs) and local egress between consecutive wakes. However, the measured persistence of ingress at high coolant flow rates was not predicted. In addition, Vaughan and Turner[11] used computational fluid dynamics (CFD) to demonstrate the effect of mainstream asymmetries, particularly their amplitude and frequency, i.e., spacing around the circumference, on the required coolant purge flow.

Radial clearance rim seals under nonwhirling, rotor-casing eccentricity conditions, e.g., caused by nonuniform thermal growth and the stack-up of fabrication/assembly tolerances, interacting with the mainstream were numerically studied by Guo and Rhode,[12] using a three-dimensional CFD code. It was found that large amounts of both mass ingress and mass egress occur between $\theta = -30$ and 100 deg, which encompasses the circumferential location of the maximum radial clearance at $\theta = 0$ deg. In addition, a 77% increase of blade root temperature was found, e.g., for a rotor eccentricity of only 7.5%.

For axial clearance rim seals, there are several CFD solutions of the simplified subproblem of an axisymmetric mainstream that excludes vanes and blades. Ko and Rhode[13] were apparently the first to show the general significance of a gap recirculation zone (GRZ) for heat transport across the rim seal, although important details were not explored. The GRZ is illustrated by the streamlines in Fig. 2 for the nominal case, except that an enlarged rim seal clearance of $c/R = 0.0187$ is used here for enhanced visibility reasons. At the nominal clearance of $c/R = 0.0094$, the GRZ is much smaller, and thus, is more difficult to observe. Note in Fig. 2 that the rim seal egress exits the cavity as an extremely thin layer passing outward on the stator shroud side of the clearance, whereupon it is abruptly swept downstream by the much faster mainstream flow.

The τ_{rx} shear stress exerted by the mainstream on the exiting egress layer at $r/R = 1.0$, and in turn, from the egress to the outer GRZ fluid near $r/R = 0.99$, serves to drive the counterclockwise motion of the GRZ. The streamlines further show that the following facts occur at the present near-nominal engine conditions:

1) The purge-coolant flow jet is unfortunately deflected away from the critically important blade root/retainer region of the rotor by the radially inward flow within the GRZ.

2) There is no mainstream mass ingress for the simplified axisymmetric subproblem solutions.

3) The GRZ exhibits a high temperature and is the mechanism that transports heat from the mainstream through the rim seal clearance.

This GRZ was also computed by Chew et al.[10] and Bohn et al.,[14] although it did not occur in the Bohn et al. laser Doppler anemometry measurements (without guide vanes). Perhaps this is caused by Bohn et al.'s operating conditions being considerably different. Further, it was found by Ko et al.[15] that the GRZ does not occur for a rim seal axial clearance equal to one-fourth of the nominal value. Consequently, at such reduced seal axial clearances, the temperature of the hottest location on the rotor drops sharply with increasing purge flow, in contrast to the nominal clearance case.

In summary, the effect of various aspects of the mainstream has been included in several rim seal studies; however, none have included all of the effects, i.e., that of blades, vanes, rotor–casing eccentricity, and various mainstream asymmetries. The great majority of the rotor–stator cavity papers have used the subproblem concept, and, thus, have excluded the mainstream flow altogether.

For axial clearance rim seals, important questions that have not been previously analyzed, which are the focus of the present work, concern, e.g., the cause–effect relationship between the high mainstream velocity and the high heat ingress, in the absence of mass ingress, for different axial clearances. Another important unanswered question concerns the conditions for which the blade-root/disk temperature is dominated by heat ingress vs disk frictional heating. A further question involves how the relative magnitudes of Re_θ and C_w affect the blade-root/disk temperature under different near-nominal operating conditions. The subsequent sections entitled, "Re_θ Effect on

Heating'' and "Combined Effect of Re_θ and C_w,'' provide answers to these lingering questions. Like other studies that exclude the mainstream, the present study uses the subproblem approach and gives an incomplete, but yet clearer understanding of certain aspects of the extremely complicated complete problem.

The next section explains the objective, and the following one discusses the two-scale k-ε turbulence model used. Subsequent sections give comparisons with related experiments, discussion of the operating conditions, results, and then a summary.

Objective

The objective is to examine, for the simple axisymmetric subproblem of an axial-clearance rim seal, important details of the transport of heat ingress in the absence of mass ingress. Of specific interest is how, and for what conditions, the heat ingress dominates over disk frictional heating for an axisymmetric rim seal and mainstream. In addition, the combined effects of Re_θ and C_w on the turbine disk temperature and the disk torque coefficient are of interest at engine operating temperatures, pressures, and flow rates. Adiabatic walls will be used in the two-dimensional axisymmetric numerical study to isolate the ingress and frictional heating effects from that of the complicated cavity-wall heat convection.

For enhanced clarity, an improved understanding of the complicated, complete problem is found from studying the simpler two-dimensional axisymmetric subproblem, which excludes all asymmetries such as that of blades and vanes. Note that the present investigation does not assume that the poorly understood complete problem can be modeled as two-dimensional axisymmetric. This approach is analogous to the case of obtaining an enhanced understanding of the complete problem of combusting airflow by studying, for simplicity reasons, the noncombusting cold flow subproblem.

Numerical Model

A finite volume computer code was used to solve the complete elliptic form of the two-dimensional, axisymmetric Navier–Stokes equations for compressible, turbulent flow. The continuity, momentum, and energy (stagnation enthalpy) equations are, respectively,

$$\frac{\partial(\rho U_i)}{\partial x_i} = 0 \tag{1}$$

$$\frac{\partial(\rho U_i U_j)}{\partial x_i} = \frac{-\partial p}{\partial x_j} + \frac{\partial \tau_{ij}}{\partial x_i} \tag{2}$$

$$\frac{\partial(\rho U_i H)}{\partial x_i} - \frac{\partial}{\partial x_j}\left(\Gamma_H \frac{\partial H}{\partial x_j}\right) = \frac{\partial}{\partial x_j}\left[U_l \tau_{lj} - \Gamma_H \frac{\partial}{\partial x_j}\left(\frac{V^2}{2}\right)\right] \tag{3}$$

The primitive variables are solved on a system of three staggered grids using the SIMPLER algorithm of Patankar.[16] The QUICK differencing scheme developed by Leonard[17] is utilized for all convective terms in the momentum equations to reduce false diffusion. This differencing scheme was implemented in a special way by Rhode et al.,[18] which promotes numerical stability. For the iteration convergence criterion, the sum of the magnitude of the normalized residuals for each cell was less than 0.001.

Turbulence Model

The high Reynolds number, i.e., standard, k-ε turbulence model[19] has been utilized in numerous previous cavity flow computations. This model gave good agreement[20] with measurements of rotor–stator cavity flows if the near-wall mesh spacing y^+ is 1) small enough to resolve the peak of radial velocity occurring there and 2) in the lower y^+ portion of the logarithmic range. The present study considers Re_θ values of 3.81×10^6, 7.1×10^6, and 11.43×10^6. The near-wall y^+ values generally covered the range between ~50 and 200.

Because there is an anticipated abrupt change in the turbulence time scales when the purge flow exits the rim seal and mixes with the mainstream, the two-scale k-ε model, recently derived and tested by Ko and Rhode,[21] was utilized in the present computations. It has been tested over a very wide range of standard test cases as well as specifically for rotor–stator cavities.[13] The superiority over the standard k-ε model occurs when there is an abrupt change in the shear field or when two flow streams dominated by different length scales mix. The latter situation occurs when the mainstream and the cavity purge flow meet at the rim seal interface.

Conventional k-ε models are based on the assumption that in all flow situations each turbulence quantity has a frequency spectrum of universal form that can be characterized by the scales of the energy-containing frequency range, i.e., large eddies. The description of the structure of a turbulent flow using a single average length scale implies that there is a constant relationship between the energy-containing length scale and the energy-dissipating length scale. For many turbulent flows, these scales do not maintain a constant proportionality, and it is for these flows that conventional versions of the k-ε model fails. Measurements indicate that large-scale turbulence eddies are much larger and exhibit a much different rate of development than do small-scale turbulence (dissipation) eddies. Therefore, the more sophisticated two-scale type of k-ε model discretizes the turbulence energy spectrum into two eddy sizes, each having its own time scale. This allows each of the two discretized eddy sizes to respond at a different rate to sudden changes in the time-mean flowfield.

The derivation of the important turbulence energy transfer rate equations begins with a different fundamental equation than that of the previous two-scale models by Fabris et al.[22] and Chen and Guo.[23] This approach circumvents the prior troublesome need to model the algebraic form of the source/sink terms of the dissipation equation using merely physical/dimensional reasoning. Also, the use of the generalized von Kármán expression for the specific turbulence energy spectrum incorporates new two-point correlation physics.

The large- and intermediate-eddy partial turbulence energies that are found in the production and transfer zones of the wave number spectrum are $k^{(1)}$ and $k^{(2)}$. The governing equations for these are, respectively,

$$\frac{Dk^{(1)}}{Dt} = P - \varepsilon^{(1)} + \text{Diff} \tag{4}$$

$$\frac{Dk^{(2)}}{Dt} = \varepsilon^{(1)} - \varepsilon^{(2)} + \text{Diff} \tag{5}$$

The transport equations for the energy transfer rates $\varepsilon^{(1)}$ and $\varepsilon^{(2)}$, which are the fluxes leaving the large- and intermediate-eddy zones, are

$$\frac{D\varepsilon^{(1)}}{Dt} = C_1^{(1)} \frac{\varepsilon^{(1)} P}{k^{(1)}} - C_2^{(1)} \frac{\varepsilon^{(1)2}}{k^{(1)}} + \text{Diff} \tag{6}$$

$$\frac{D\varepsilon^{(2)}}{Dt} = C_1^{(2)} \frac{\varepsilon^{(2)2}}{k^{(2)}} + C_2^{(2)} \frac{\varepsilon^{(1)}\varepsilon^{(2)}}{k^{(2)}} + C_3^{(2)} \frac{\varepsilon^{(2)} P}{k^{(2)}} - C_4^{(2)} \frac{\varepsilon^{(2)} P}{k^{(1)}} - C_5^{(2)} \frac{\varepsilon^{(1)}\varepsilon^{(2)}}{k^{(1)}} + \text{Diff} \tag{7}$$

Observe that $k = k^{(1)} + k^{(2)}$, and that the turbulent viscosity is obtained from

$$\nu_t = \frac{C_\mu (k^{(1)} + k^{(2)})^2}{\varepsilon^{(2)}} \tag{8}$$

Because the mainstream effect considered occurs only at the rim seal, only the extremely narrow axial space corresponding to the narrow wheelspace cavity has been modeled herein. Figure 1 illustrates the idealized cavity showing the computational domain. Only the radially thin, inner portion of the mainstream duct was included in the computational domain, as the freestream boundary conditions were specified at the radially outer surface of the (mainstream) domain. Specifically, 1) the axial and swirl velocities were fixed at the freestream nominal values, 2) the radial velocity was given a zero value, and 3) most others were given a zero radial gradient. A series of preliminary solutions was obtained wherein the radial height of the portion of the mainstream included in the computational domain was reduced by about half each time, until only a 4% change on the thermal distributions was observed. The resulting thickness of the radially inner portion of the mainstream in the domain was utilized for the production computations.

In modeling the mainstream duct, an experienced turbine designer‡ was consulted. Particularly because only the short axial clearance gap of the rim seal is of interest here, it was decided that approximating the duct using nondiverging, i.e., constant radius, walls is a good approximation. The justification for this approximation is the fact that the effect of the diverging flow path in an actual turbine is largely counterbalanced by the increasing boundary-layer displacement thickness, which is caused by the mainstream swirl velocity. Further, several preliminary solutions, each with a different mainstream domain outlet axial location, were examined in choosing the preferred outlet location.

Boundary Conditions

Actual engine nominal flow parameters, as supplied by Ivey,§ were utilized to specify inlet values of axial and tangential velocity, as well as enthalpy, temperature, and pressure at both inlets. The turbulence kinetic energy was assumed equal to an extremely small percentage of the mean flow kinetic energy. This value was then split between the partial energies $k^{(1)}$ and $k^{(2)}$, according to the ratio $k^{(1)}/k^{(2)} = 1.5$. This ratio was obtained from trial and error numerical experiments, e.g., for a flat-plate boundary layer. Inlet values of $\varepsilon^{(1)}$ and $\varepsilon^{(2)}$ were estimated from:

$$\varepsilon^{(1)} = \varepsilon^{(2)} = k^{1.5}/L_e \tag{9}$$

where L_e for each inlet passage was assumed equal to 30% of the respective passage radial width. The equality of turbulence energy transfer rates is based on the Kolmogorov equilibrium theorem resulting in an equilibrium shape for the turbulence energy spectrum. Kim and Chen[24] found that the assumed spectrum shape at the inlet did not have a significant effect on the mean flow solution.

At the domain outlet, the axial velocity was corrected for each iteration to achieve global mass conservation. Further, as mentioned earlier, adiabatic walls were specified on all solid surfaces so that fluid heating would indicate the thermal transport from the mainstream or disk frictional heating. In addition, standard wall functions[19] were utilized along walls to avoid computing through the low-Reynolds number region for both the radial and swirl momentum equations. The turbulence energy transfer quantities $\varepsilon^{(1)}$ and $\varepsilon^{(2)}$ were evaluated at the near-wall grid points from the usual expression:

$$\varepsilon^{(1)} = \varepsilon^{(2)} = C_\mu^{0.75} k^{1.5}/\kappa y \tag{10}$$

where y is the normal distance from the wall.

The highly nonuniform grids were single-block in nature, with a coarse grid in the center of the cavity and contracting to a fine grid spacing along all walls. Grid-sensitivity tests were conducted using several grids. The grid of 104 × 144 lines (axially and radially) gave a sensibly grid-independent solution and was utilized for the production computations. Specifically, this grid gave less than a 4% change in the local quantities of interest, compared to that with 60 × 117 lines. All grids had a constant near-wall grid spacing of 0.242 mm to ensure that the wall function gave, as nearly as possible, the same wall values.

Comparison with Experiment

Predictions using the two-scale k-ε model have previously been compared[13] with the radial and circumferential velocity measurements by Daily et al.,[25] as well as the standard k-ε model solution, for a similar rotating cavity with axial purge inlet flow and radial outlet flow. Predictions by Chew and Vaughan,[26] using the Prandtl mixing-length turbulence model, were also available for the radial velocity comparison. The two-scale model (presently used) generally gave more realistic solutions than the other two models. Additional comparisons also show the preference for the two-scale model for the entire throughflow parameter $C_w = Q/(\nu R)$ range from 1450 to 3443, and for the $Re_\theta = \Omega R^2/\nu$ range from 2.95×10^5 to 9.5×10^6. Of particular interest is the comparison[13] with measurements of the disk friction moment coefficient[25] for Re_θ ranging from 2.5×10^6 to 9.5×10^6. The present two-scale solution showed a discrepancy of ~7%, whereas the standard k-ε solution showed 27% discrepancy.

An additonal comparison with measurements is found in Figs. 3a and 3b. These figures show comparisons between the present two-scale predictions and the measurements[25] of radial and swirl velocity at each of three different radial stations. The level of agreement of the two-scale solution with measurements improves with increasing r/R, particularly for the radial

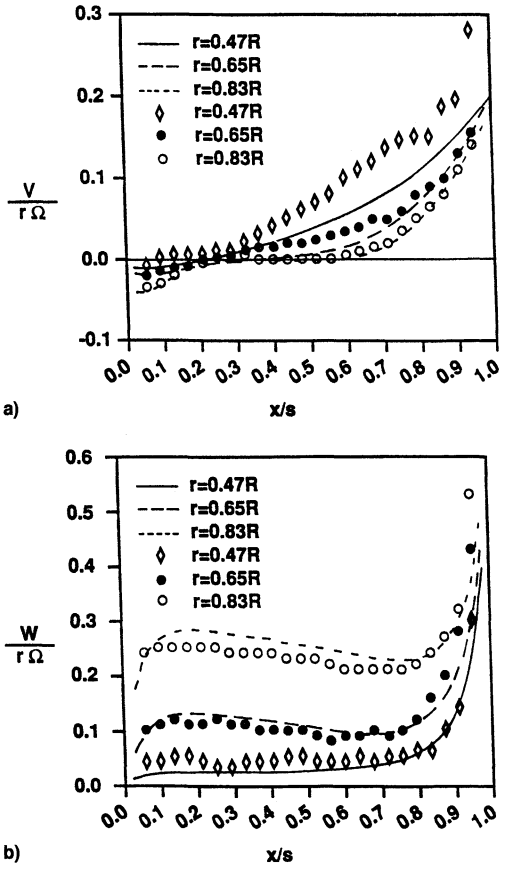

Fig. 3 Predicted a) radial and b) tangential velocity distributions for enclosed rotating disks with throughflow (curves are present predictions; symbols are meaurements of Daily et al.[25]). $C_w = 1708$, $Re_\theta = 6.95 \times 10^5$.

‡Baskharone, E., private communication, 1990.
§Ivey, P., private communication, 1990.

velocity. In addition, the historically defying test case of a free axisymmetric jet was also considered. The standard k-ε model overpredicted the measured spreading rate of the jet by 23%, whereas the present two-scale model overpredicted it by only 18%.

Discussion

The physical dimensions of the generalized cavity considered are radius of the rotor R = 0.3078 m, radial width of the mainstream passage H/R = 0.0975, axial width of the cavity s/R = 0.0612, axial width of the rim seal c/R = 0.00936, radial width of the cavity inlet a/R = 0.00725, radial location of the cavity inlet R_i/R = 0.795, and radial thickness of the shroud t/R = 0.00725. The cooling flow enters the cavity axially through an annular slit in the stator at temperature T_2 and leaves radially through the axial gap between the rotor and the stator shroud extended from the stator.

Typical engine nominal flow parameters according to Ivey§ are 1) axial Reynolds number in the main pass $Re_{x,m} \equiv (2\rho UH)/\mu = 1.17 \times 10^6$; 2) rotational Reynolds number of the rotor $Re_\theta \equiv (\rho\Omega R^2)/\mu = 7.62 \times 10^6$; 3) cooling flow rate $C_w \equiv Q/(\nu R) = 7100$; 4) differential pressure $\Delta P^* \equiv [(P_2 - P_1)/P_1] \times 10^3 = -10$; 5) differential temperature $\Delta T^* \equiv 2C_p(T_2 - T_1)/(\Omega R)^2 = -4.6$; 6) swirl ratio at the main pass domain inlet $W/U = \tan(\pi/12)$; and 7) swirl ratio at the turbine cavity domain inlet $W/U = 0$. Subscripts 1 and 2 refer to the mainstream and the cooling purge flow, respectively. The fluid properties above are evaluated at T_1 and P_1.

Pressure Distribution

The pressure field corresponding to Fig. 2 is given in Fig. 4, where the values shown are relative to the mainstream inlet values as shown. The cavity swirl velocity gives the expected higher pressure at the outer portion of the cavity. Note that a local increase of pressure on the rotor near r/R = 0.92 occurs, indicating the radially inner stagnation point of the GRZ. In addition, there is a sharp pressure peak at the stagnation point near the outer edge of the rotor where the mainstream impacts it. This is seen more clearly in the magnified view of the relative pressure in Fig. 5.

Rim Seal Turbulence

Our understanding of the turbulent heat diffusion across the mainstream-rim seal interface is enhanced from studying the turbulence kinetic energy distribution for the case of Figs. 2, 4, and 5, which is shown in Fig. 6. The dimensionless quantity has been magnified by the factor of 400 for graphical convenience. The typical magnified dimensionless turbulence energy is near 0.4, except near the GRZ, which exhibits values up to about 12 near the mainstream interface. Such extremely high interface values indicate intense instantaneous mixing of turbulent eddies transporting momentum and heat, which is particularly enhanced by the extremely large radial gradient of the local axial velocity and temperature at this location. Specifically, because of the intense generation of turbulence kinetic energy at the interface, highly turbulent eddies instantaneously exchange heat 1) from the hot mainstream to the thin, exiting egress layer; 2) then from the egress layer to the GRZ near r/R = 0.99; and 3) from the GRZ to the outer blade root surface near r/R = 0.98 (for the actual nonadiabatic case), as well as to the coolant-purge layer flowing radially outward alongside the GRZ. Recall that the design goal was that the coolant fluid

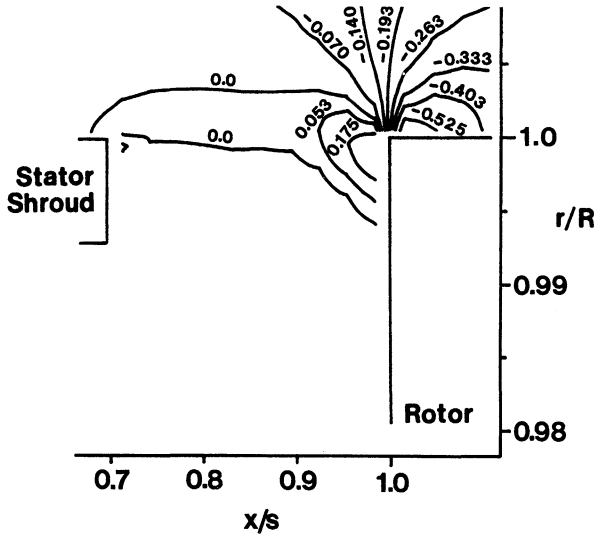

Fig. 5 Magnified view of pressure contours near the rim seal interface for c/R = 0.0187.

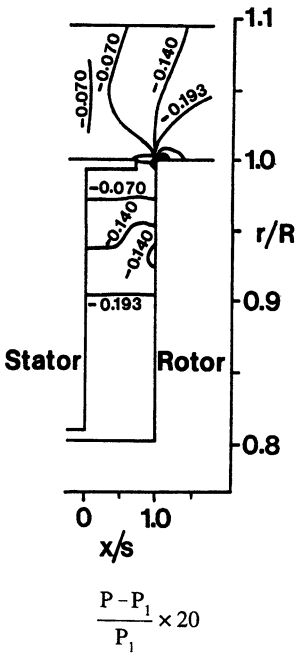

Fig. 4 Pressure contours for the entire domain.

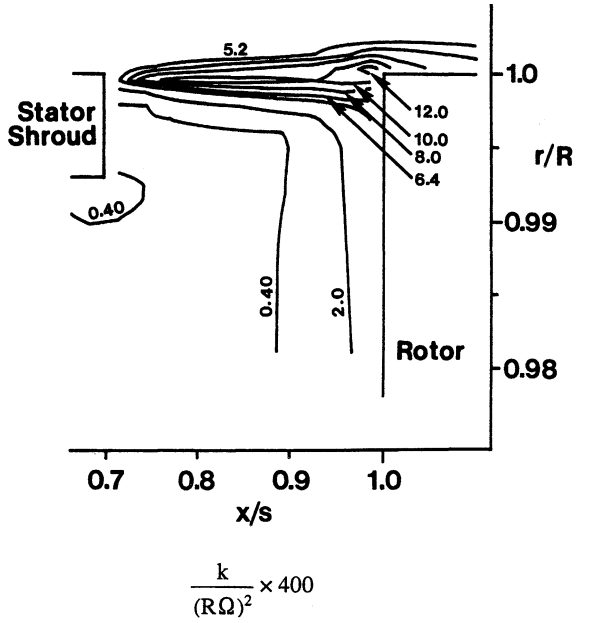

Fig. 6 Magnified view of turbulence kinetic energy near the rim seal interface for c/R = 0.0187.

would cool the blade root. Thus, one can now appreciate how the intense τ_{rx} shear stress at the interface gives a large local turbulence generation rate, which in turn, produces a large turbulence energy, and thus, a locally large turbulent radial heat diffusion. As a result of further mixing within the GRZ, one expects to find that the entire GRZ exhibits a fairly high temperature compared with the cavity-average temperature.

Turbulence energy contours for the case of engine nominal rim seal axial clearance $c/R = 0.0094$ are shown in Fig. 7. This smaller axial clearance gives less particle transit time for turbulence energy generation and for the egress layer to receive momentum and heat diffusion from the mainstream and, in turn, to diffuse them to the GRZ. Thus, Fig. 7 shows reduced levels of turbulence energy near the interface and along the rotor. As expected, the reduced particle transit time also gives reduced recirculation velocities within the GRZ, which exhibits less inward radial momentum on the rotor, and thus, a smaller area for heat convection near the blade root surface for the actual, i.e., nonadiabatic case.

Re_θ Effect on Heating

For nominal C_w and rim seal axial clearance, the radial distribution of disk adiabatic temperature is shown in Fig. 8 for the nominal, 50% increased, and 50% decreased Re_θ, i.e., rpm, cases. Recall that all surfaces were treated as adiabatic so that the cavity heating is solely from mainstream diffusion and disk friction effects. Observe that the expected large, abrupt jump of disk temperature occurs at the inner extremity of the hot GRZ. Compared with the larger clearance case of Fig. 2, the present nominal clearance gives a reduced GRZ recirculating velocity in opposition to the centrifugal pumping, and therefore, the inner extremity is found at the slightly outer radial location of $r/R = 0.98$ for the nominal $Re_\theta = 7.62 \times 10^6$. The slope of the inner portion of each temperature distribution indicates the disk frictional heating effect on the centrifugally pumped disk layer of outward flowing coolant. The local temperature maximum occurs at the inner extremity of the GRZ, especially for the higher Re_θ cases, because this location is a stagnation point with a locally higher stagnation temperature. Further, note that each Re_θ case has approximately the same temperature jump as a result of the mainstream-to-GRZ heat diffusion; however, each has a significantly different GRZ temperature. This is attributed to the fact that the high GRZ temperature approximately equals the temperature increase from disk frictional heating plus that from mainstream diffusion to the GRZ. Thus, the low Re_θ (low disk speed) gives a low GRZ temperature because of low disk frictional heating, and similarly, the high Re_θ gives a high GRZ temperature.

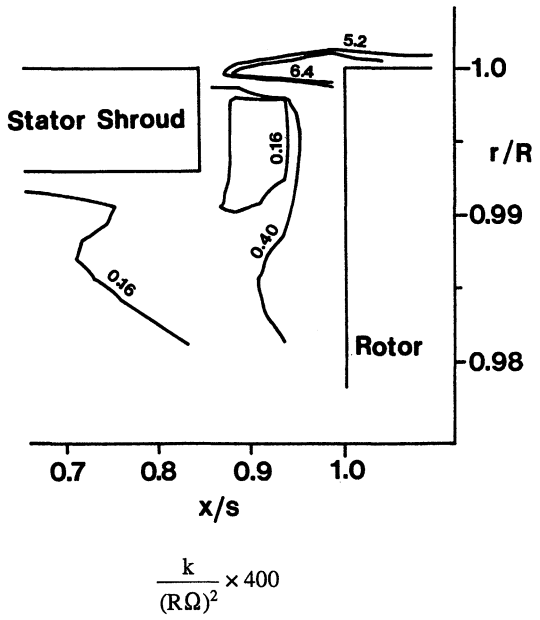

Fig. 7 Magnified view of turbulence kinetic energy near the rim seal interface for $c/R = 0.0094$.

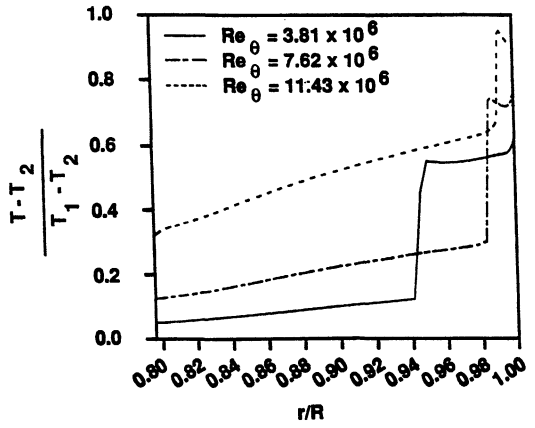

Fig. 8 Effect of the tangential Reynolds number on the adiabatic temperature distribution along the rotor surface for $C_w = 7200$.

Combined Effect of Re_θ and C_w

For the generalized configuration specified, the results in Fig. 9 show the predicted maximum disk surface (adiabatic) temperature for various C_w and Re_θ. Because the maximum temperature often occurs at essentially the blade root location, this temperature is often a primary concern in designing the cavity. As mentioned earlier, the maximum rotor temperature is the adiabatic stagnation temperature occurring at the radially inner stagnation point of the GRZ. As shown in Fig. 9, 1) T_{max} decreases significantly and monotonically as the purge flow C_w increases and 2) as Re_θ increases, T_{max} becomes increasingly sensitive to Re_θ. Item 2 indicates that disk frictional heating becomes more important relative to heat ingress as Re_θ increases above the nominal Re_θ value of 7200. Observe that T_{max} is quite high, even greater than T_1, for $C_w = 1500$ and $Re_\theta = 11.43 \times 10^6$. This is because this operating condition gives 1) maximum disk frictional heating, 2) maximum ingress heating of the overall cavity (maximum GRZ size), and 3) minimum cooling.

For the case of low $Re_\theta = 3.81 \times 10^6$, Fig. 10 shows the effect on disk temperature of C_w values that are 1) nominal, 2) 50% increased, and 3) 50% decreased. Overall, these cases give low frictional heating and low outward radial momentum on the disk, i.e., a relatively large GRZ. Hence, a small disk temperature slope and relatively cool overall temperatures are found.

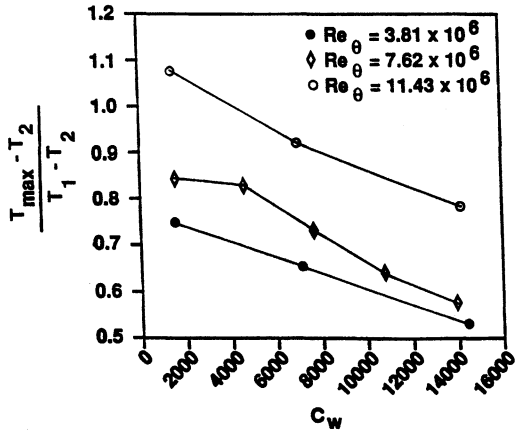

Fig. 9 Effect of the cooling flow rate C_w at each Re_θ on the maximum adiabatic temperature along the rotor surface.

The three C_w cases at the high Re_θ value of 11.4×10^6 are shown in Fig. 11. Here one finds the expected large disk frictional heating effect. Compared with the low Re_θ cases in Fig. 10, a reduction in the temperature jump magnitude at the GRZ inner stagnation point is found. This results from 1) larger disk frictional heating giving a larger temperature on the inward side of the GRZ inner stagnation point, and 2) somewhat invariant ingress heating. Also, the effect of increasing C_w exhibits a smaller effect on the size of the GRZ here than in Fig. 10 because the larger centrifugal pumping reduces the GRZ to a small size regardless of the C_w value.

Combined Effect of Re_θ and C_w on C_m

Figure 12 shows the combined effects of Re_θ and C_w, over a wide range, on the friction moment coefficient, $C_m \equiv M/(0.5\rho\Omega^2R^5)$. Note that C_m is increasingly sensitive to Re_θ as Re_θ is increased above the engine nominal value. Also notice that C_w has a negligible effect on the moment coefficient. Because of the large $\tau_{x\theta}$ tangential wall shear stress, a small change in the τ_{xr} radial wall shear stress caused by a change of C_w is too small to affect the total frictional moment M.

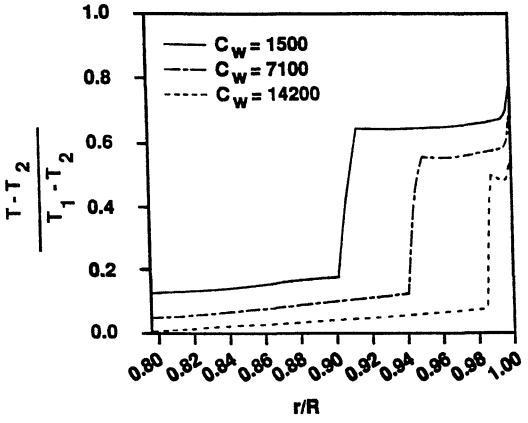

Fig. 10 Effect of the cooling flow rate C_w on the adiabatic temperature distribution along the rotor surface for $Re_\theta = 3.81 \times 10^6$.

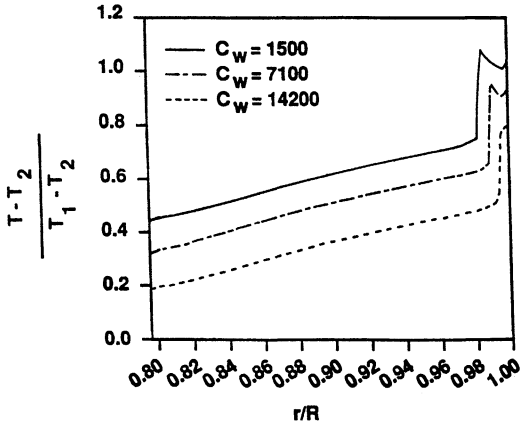

Fig. 11 Effect of the cooling flow rate C_w on the adiabatic temperature distribution along the rotor surface for $Re_\theta = 11.4 \times 10^6$.

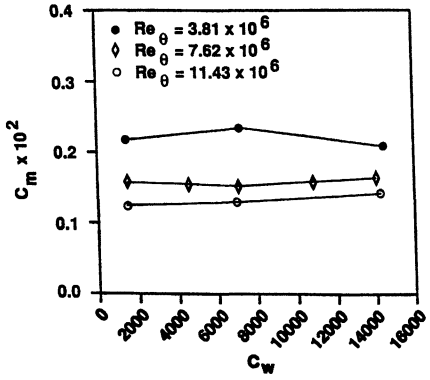

Fig. 12 Effect of the cooling flow rate C_w at each Re_θ on the frictional moment coefficient.

Summary

For the simple subproblem of an axisymmetric mainstream, the present (first) examination of the rim seal turbulent kinetic energy distribution, and its role in diffusing mainstream heat to the disk, provide an enhanced understanding of blade-root/disk heating. Also, the combined effects of Re_θ and C_w on the blade-root/disk adiabatic temperatures were investigated. Wall heat convection of the entire rotor–stator cavity was eliminated by specifying adiabatic walls for all surfaces. Realistic temperatures, pressures, and flow rates were strictly used in accordance with commercial engine nominal flow parameters. Complete momentum and thermal effects were included in the elliptic, two-dimensional axisymmetric Navier–Stokes solutions.

For the present axial clearance rim seal at nominal conditions, significant heat ingress with no mass ingress was found in the two-dimensional axisymmetric solutions. Specific current findings are as follows:

1) The high blade-root/disk adiabatic temperature depends largely on the extremely high-turbulence kinetic energy of the rim seal-mainstream interface, which is generated by the intense τ_{rx} from the mainstream.

2) The turbulent heat diffusion ingress from the mainstream is dominant over the disk frictional heating for Re_θ values near half of the engine nominal value.

3) An increased rim seal axial clearance provides greater turbulence generation, which produces increased ingress heat diffusion.

4) High values of Re_θ give a high GRZ temperature but sufficient centrifugal pumping to reduce the GRZ area for disk heat convection near the blade root surface.

5) In addition to cooling, high values of C_w reduce the GRZ area for disk heat convection near the blade root surface.

6) The disk torque coefficient is almost independent of the coolant flow, but is increasingly sensitive to Re_θ, as Re_θ increases above the nominal value.

7) The maximum rotor temperature, which is near the blade root, is even higher than the mainstream temperature for high Re_θ and low C_w.

Acknowledgments

The financial support of the Turbomachinery Research Consortium of Texas A&M University is gratefully acknowledged. The authors are also indebted to the Supercomputer Center of Texas A&M University for a grant of Cray Y-MP CPU time. The technical information supplied by P. Ivey and E. Baskharone is greatly appreciated.

References

[1]Phadke, U. P., and Owen, J. M., "Aerodynamic Aspects of the Sealing of Gas Turbine Rotor-Stator Systems, Part 1: The Behaviour of Simple Shrouded Rotating Disk Systems in a Quiescent Environment," *International Journal of Heat and Fluid Flow*, Vol. 9, 1988, pp. 98–105.

[2]Phadke, U. P., and Owen, J. M., "Aerodynamic Aspects of the Sealing of Gas Turbine Rotor-Stator Systems, Part 2: The Performance of Simple Seals in a Quasi-Axisymmetric External Flow," *International Journal of Heat and Fluid Flow*, Vol. 9, 1988, pp. 106–112.

[3]Phadke, U. P., and Owen, J. M., "Aerodynamic Aspects of the Sealing of Gas Turbine Rotor-Stator Systems, Part 3: The Effect of Non-Axisymmetric External Flow on Seal Performance," *International Journal of Heat and Fluid Flow*, Vol. 9, 1988, pp. 113–117.

[4]Campbell, D. A., "Gas Turbine Disc Sealing System Design," *AGARD Conference on Seal Technology in Gas Turbine Engine*, AGARD, CP-237, 1978.

[5]Abe, T., Kikuchi, J., and Takeuchi, H., "An Investigation of Turbine Disc Cooling (Experimental Investigation and Observation of Hot Gas Flow into a Wheelspace)," 3rd CIMAC Conf., Paper GT-30, 1979.

[6]Kobayashi, N., Matsumoto, M., and Shizuya, M., "An Experimental Investigation of a Gas Turbine Disk Cooling System," *Journal of Engineering for Gas Turbines and Power*, Vol. 106, 1984, pp. 136–141.

[7]Dadkhah, S., Turner, A. B., and Chew, J. W., "Performance of Radial Clearance Rim Seals in Upstream and Downstream Rotor-Stator Wheelspaces," *Journal of Turbomachinery*, Vol. 114, 1992, pp. 439–445.

[8]Hamabe, K., and Ishida, K., "Rim Seal Experiments and Analysis of a Rotor-Stator System with Nonaxisymmetric Main Flow," International Gas Turbine Aeroengine Congress and Exposition, American Society of Mechanical Engineers, Paper 92-GT-160, June 1992.

[9]Owen, J. M., and Rogers, R. H., *Flow and Heat Transfer in Rotating Disk Systems, Vol. 1: Rotor-Stator Systems*, Wiley, New York, 1989.

[10]Chew, J. W., Green, T., and Turner, A. B., "Rim Sealing of Rotor-Stator Wheelspaces in the Presence of External Flow," International Gas Turbine Aeroengine Congress and Exposition, American Society of Mechanical Engineers, Paper 94-GT-126, June 1994.

[11]Vaughan, C. M., and Turner, A. B., "Numerical Prediction of Axisymmetric Flow in a Rotor-Stator System with an External Mainstream Flow," *Proceedings of the 5th International Conference on Numerical Methods in Laminar and Turbulent Flows*, Pineridge, Swansea, Wales, UK, 1987, pp. 1640–1651.

[12]Guo, Z., and Rhode, D. L.,"Computed Eccentricity Effects on Turbine Rim Seals at Engine Conditions with a Mainstream," *Journal of Turbomachinery*, Vol. 118, Jan. 1996, pp. 143–152.

[13]Ko, S. H., and Rhode, D. L., "Thermal Details in a Rotor-Stator Cavity at Engine Conditions with a Mainstream," *Journal of Turbomachinery*, Vol. 114, 1992, pp. 446–453.

[14]Bohn, D., Johann, E., and Kruger, U., "Experimental and Numerical Investigations of Aerodynamic Aspects of Hot Gas Ingestion in Rotor-Stator Systems with Superimposed Cooling Mass Flow," International Gas Turbine Aeroengine Congress and Exposition, American Society of Mechanical Engineers, Paper 95-GT-143, June 1995.

[15]Ko, S. H., Rhode, D. L., and Guo, Z., "Circumferentially-Smeared Computed Effects of Rim Seal Clearance on Wheelspace Thermal Distributions," *Journal of Turbomachinery*, Vol. 119, 1997, pp. 157–159.

[16]Patankar, S. V., *Numerical Heat Transfer and Fluid Flow*, McGraw–Hill, New York, 1980.

[17]Leonard, B. P., "A Stable and Accurate Convective Modelling Procedure Based on Quadratic Upstream Interpolation," *Computer Methods in Applied Mechanics and Engineering*, Vol. 19, 1979, pp. 59–98.

[18]Rhode, D. L., Demko, J. A., Traegner, U. K., Morrison, G. L., and Sobolik, S. R., "Prediction of Incompressible Flow in Labyrinth Seals," *Journal of Fluids Engineering*, Vol. 108, 1986, pp. 19–25.

[19]Launder, B. E., and Spalding, D. B., "The Numerical Computation of Turbulent Flows," *Computational Methods in Applied Mechanics and Engineering*, Vol. 3, 1974, pp. 269–289.

[20]Virr, G. P., Chew, J. W., and Coupland, J., "Application of Computational Fluid Dynamics to Turbine Disc Cavities," International Gas Turbine Aeroengine Congress and Exposition, American Society of Mechanical Engineers, Paper 93-GT-89, May 1993.

[21]Ko, S. H., and Rhode, D. L., "Derivation and Testing of a New Multi-Scale k-ε Turbulence Model," AIAA Paper 90-0243, Jan. 1990.

[22]Fabris, G., Harsha, P. T., and Edelman, R. B., "Multiple-Scale Turbulence Modeling of Boundary Layer Flows for Scramjet Applications," NASA CR-3433, 1981.

[23]Chen, C. P., and Guo, Kuan-ling, "A Non-Isotropic Multi-Scale Turbulence Model," *Applied Mathematics and Mechanics*, English edition, Vol. 12, No. 10, 1991, pp. 981–991.

[24]Kim, S. W., and Chen, C. P., "A Multiple-Time-Scale Turbulence Model Based on Variable Partitioning of Turbulent Kinetic Energy Spectrum," NASA CR-179222, 1987.

[25]Daily, J. W., Ernst, W. D., and Asbedian, V. V.,"Enclosed Rotating Disks with Superposed Through Flow: Mean Steady and Periodic/Unsteady Characteristics of the Induced Flow," Hydrodynamics Lab., Massachusetts Inst. of Technology, Rept. 64, Cambridge, MA, 1964.

[26]Chew, J. W., and Vaughan, C. M., "Numerical Predictions for the Flow Induced by an Enclosed Rotating Disc," International Gas Turbine Aeroengine Congress and Exposition, American Society of Mechanical Engineers, Paper 88-GT-127, June 1988.